Supporting Information

Zuccotti et al. 10.1073/pnas.1320290111

SI Materials and Methods

Plasmid Cloning. The Fezf2 ORF was amplified by PCR from a mouse cDNA brain library and cloned into a shuttle vector using a TA Cloning Kit (Qiagen). Fezf2 was then subcloned into a lentiviral plasmid (LV) containing the ubiquitin promoter (Fubi), the internal ribosome entry site (IRES) and EGFP to generate LV-Fubi-Fezf2-IRES-EGFP. As a lentiviral control plasmid, we used LV-Fubi-IRES-tdTomato. Fezf2 was also subcloned into a retroviral Moloney murine leukemia virus (MMLV) plasmid containing the Raus sarcoma virus (RSV) promoter, T2A, and tdTomato to generate MMLV-RSV-Fezf2-T2A-tdTomato. MMLV-RSV-EGFP served as a control retroviral plasmid.

Viral Production and Injections. The packaging cell line HEK 293 was cotransfected with the viral backbone vector and the helper plasmids, and the viral particles were purified by ultracentrifugation. The concentrated viral solutions (10^6–10^8 cfu/mL) were titrated and mixed. One to two microliters of the viral solution was injected into the subventricular zone (SVZ) of pups, which were anesthetized by hypothermia, at postnatal day 4 (P4). The following coordinates from the bregma were used: 0.6 anterior, 1.2 lateral, and 1.5 ventral. To infect only neuroblasts, Fezf2 lentivirus was injected in the RMS of P8 mice, using the following coordinates from the bregma: 2.2 anterior, 0.9 lateral, and 2.7 ventral. For injection in the SVZ of adult mice, the following coordinates from the bregma were used: 0.9 anterior, 1.2 lateral, and 2.5 ventral. Fezf2-expressing viruses were always injected with the corresponding control virus (i.e., a viral vector encoding a fluorophore). The animals were placed on a heating pad and returned to their home cages. The mice were killed at different time points after injection. Electrophysiological recordings were performed 20–71 d after injection. However, the average time after virus injection in each group was similar. This time [given as days postinjection (dpi), mean ± SEM, 25th–75th percentiles] was 38.4 ± 3.4 (range: 32–39) dpi for oversized, respecified Fezf2$^+$ neurons (n = 15), 34.8 ± 4.4 (range: 20–45) dpi for small Fezf2$^+$ neurons (n = 19), and 30.9 ± 0.4 (range: 30–33) dpi for control granule cells (n = 20). One-way ANOVA confirmed that the age difference between the groups was not significant ($P > 0.05$).

Neonatal SVZ Electroporation. One to two microliters of Fezf2-EGFP and TdTomato plasmid mix was injected into the lateral ventricles of pups, which were anesthetized by hypothermia, at P2. The following coordinates from the bregma were used: 0.5 anterior, 0.8 lateral, and 2.2 ventral. Five-millimeter tweezertrodes were placed on each side of the skull after injection, and mice were subjected to five electrical pulses of 100 V (60 ms, separated by 940 ms) generated using a BTX ECM 830 Electroporator (Harvard Apparatus). For specifically electroporating the lateral or dorsal SVZ, tweezertrodes were positioned as previously described (1).

Neurosphere Preparation. The dorsal or lateral SVZ was microdissected from 500-mm thick coronal sections of P3–P4 mouse brains. The tissue was treated with papain (0.08%)/DNase I (0.001%) for 3 min at 37 °C to obtain a single-cell suspension that was cultured at a density of 100,000 cells per milliliter in B27 serum-free/Neurobasal media (Life Technology) supplemented with glutamine (2 mM), EGF (20 ng/mL), and FGF (20 ng/mL) (all from Sigma-Aldrich). Neurospheres were infected with either TdTomato or Fezf2-IRES-EGFP–expressing lentivirus at 5 days in vitro. One day after, neurospheres were allowed to differentiate into neurons on polylysine-treated coverslips in the absence of EGF and FGF. Three or 14 d after differentiation, the neurons were fixed for 10 min in 4% (wt/vol) PFA and immunostained. For electrophysiological recordings, neurons were kept in culture for 3 wk in the presence of BDNF (20 ng/mL).

Immunostaining. Animals were deeply anesthetized and perfused with 4% PFA. Brains were dissected and postfixed in 4% PFA overnight at 4 °C. Sixty-micrometer thick sections were prepared using a Leica VT100S vibratome (Leica Microsystems GmbH). Neurons were fixed for 10 min in 4% PFA. Slices/neurons were blocked in 0.2% Triton and 3–6% (wt/vol) BSA and incubated overnight with primary antibodies at 4 °C, followed by incubation with secondary antibodies at room temperature. Brain sections or neurons were stained for the following: tdTomato (rabbit anti-DsRed, 1:1,000; BD Biosciences), EGFP [chicken anti-EGFP, 1:1,000; Invitrogen (or rabbit anti-EGFP)], glutamic acid decarboxylase 67 (mouse, 1:1,000; Millipore), VGlut1 (rabbit, 1:2,000; Synaptic Systems), CRYM (mouse, 1:1,000; Abcam), βIII-Tubulin (mouse, 1:2,000; Sigma-Aldricht), tau (rabbit, 1:500; Synaptic Systems), Tbr1 (rabbit, 1:300; Abcam), and Tbr2 (rabbit, 1:250; Abcam). The following secondary antibodies were used: anti-rabbit Cy3 (1:1,000; Jackson ImmunoResearch Laboratories), anti-rabbit Alexa 647 (1:1,000; Invitrogen), anti-chicken Alexa 488 (1:1,000; Invitrogen), anti-mouse Alexa 488 (1:1,000; Invitrogen), and anti-mouse Alexa 647 (1:1,000; Invitrogen).

Single-Cell RT-PCR. For single-cell RT-PCR analysis of Vglut1 expression, the cytoplasm of Fezf2 oversized and TdTomato control neurons was aspirated into patch pipettes, which were pulled from autoclaved borosilicate glass (resistance of 1.5–2.5 MΩ, filled with autoclaved internal solution), by gentle suction under visual control. The harvested material was subsequently expelled into an autoclaved tube and stored at −80 °C. To obtain cDNA, we used SuperScript VILO MasterMix (Life Technology), following the manufacturer's instructions. Two rounds of PCR amplification were performed. The template for the second PCR amplification was 10 μL of the first PCR amplification. The following primers were used: forward, CCGGCAGGAGGAGTTTCGGAAG, and reverse, AGGGATCAACATGTTTAGGGTGGAGGTAGC, for the first PCR assay and forward, TA CTGGAGAAGCGGCAGGAAGG, and reverse, CCAGAAAAAGGAGCCATGTATGAGG, for the second PCR assay. The primer pairs were intron-overspanning to distinguish amplification of cDNA from amplification of genomic DNA. The PCR conditions were the same for both amplification rounds; after a hot start at 94 °C for 3 min, 35 cycles (94 °C for 1 min, 60 °C for 30 s, and 68 °C for 45 s) were performed. The results were analyzed on ethidium bromide-stained agarose gel. Experimental conditions were optimized using cortical pyramidal cells and interneurons as positive and negative controls, respectively.

Electrophysiology. Acute olfactory bulb slices were prepared from mice 3–10 wk after virus injection. Mice were deeply anesthetized and killed by decapitation. The brain was removed and submerged in ice-cold artificial cerebrospinal fluid (ACSF) containing 125 mM NaCl, 25 mM $NaHCO_3$, 1.25 mM NaH_2PO_4, 2.5 mM KCl, 2 mM $CaCl_2$, 1 mM $MgCl_2$, and 25 mM glucose, and it was continuously bubbled with 95% O_2 and 5% CO_2 (pH 7.3). Sagittal slices (250 μm) were cut using a vibratome (Sigmann Elektronik). Slices were kept at 32 °C for 30 min and subsequently stored at room temperature. Slices were transferred to a recording chamber

and superfused with ACSF at 30–32 °C. Whole-cell current-clamp recordings were performed using pipettes pulled from borosilicate glass capillaries with a resistance of 6–8 MΩ when filled with the following solution: 105 mM potassium gluconate, 30 mM KCl, 4 mM Mg-ATP, 10 mM phosphocreatine, 0.3 mM GTP, and 10 mM Hepes, adjusted to pH 7.3 with KOH (final osmolarity of 290 mOsm). $GABA_A$ receptors were blocked with 10 μM SR95531 hydrobromide (gabazine; Biotrend), AMPA receptors were blocked with 10 μM 6-cyano-7-nitroquinoxaline-2,3-dione (CNQX; Biotrend), and NMDA receptors were blocked with 50 μM d-2-Amino-5-Phosphonovaleric acid (d-APV Biotrend). For voltage-clamp recordings of miniature inhibitory postsynaptic currents (mIPSCs) and miniature excitatory postsynaptic currents (mEPSCs), pipettes were filled with a solution containing 120 mM cesium gluconate, 10 mM CsCl, 8 mM NaCl, 10 mM Hepes, 10 mM phosphocreatine-Na, 0.3 mM Na_3GTP, 2 mM MgATP, and 0.2 mM EGTA (pH 7.3, adjusted with NaOH). The mIPSCs were recorded in the presence of 1 μM tetrodotoxin (BIOTREND Chemicals), 10 μM CNQX, and 50 μM d-APV. The mEPSCs were recorded in the presence of 1 μM tetrodotoxin, 10 μM gabazine, and 50 μM d-APV. Stimulus delivery and data acquisition were performed using PatchMaster (HEKA). Signals were sampled at 10 kHz and filtered at 3 kHz, and off-line analysis was performed using Igor Pro (WaveMetrics) and PClamp (Molecular Devices).

To test response currents in SVZ-derived neurons, the cells were step-depolarized for 1 ms, from −70 mV to +30 mV in voltage-clamp condition. Blockers (CNQX or gabazine) were applied singularly to different $Fezf2^+$ cells (seven of seven $Fezf2^+$ cells were blocked by CNQX; five of five $Fezf2^+$ cells were blocked by gabazine).

Morphological Reconstruction. Neurons were filled with biocytin (~0.5%) added to the intracellular pipette solution. Slices were postfixed and quenched in 1% (vol/vol) H_2O_2, followed by incubation with avidin–biotin–HRP complex (Elite ABC; Vector Laboratories). The immunoperoxidase reaction was developed using 3,3′-diaminobenzidine (DAB, Sigma-Aldrich) as a chromogen. Three-dimensional neuronal reconstructions, dendritic length, and dendritic branching analyses were performed using the Neurolucida software package (MBF Bioscience).

Image Acquisition, Quantification, and Statistical Analysis. Images were acquired using a Zeiss (LSM 700) confocal microscope and analyzed with Zen software (Carl Zeiss). For cell body size assessment, we measured control and Fezf2-expressing cells in an 800 × 800-μm square randomly applied in the olfactory bulb from five to seven coronal slices per bulb. For neuronal marker quantification in cultured neurons, three coverslips from three separated experiments were stained for each marker. On each coverslip, three images were acquired and the number of marker-positive cells was counted.

Statistical analyses were performed with GraphPad Prism 5 software. We used the two-tailed *t* test, one-way ANOVA (followed by Tukey's post hoc test), and two-way ANOVA (followed by Bonferroni multiple comparison post hoc analysis) to compare normally distributed data. We used the Mann–Whitney test and the Kruskal–Wallis test (followed by Dunn's multiple comparison post hoc analysis) to compare nonnormally distributed data. Cumulative distributions were compared using the Kolmogorov–Smirnov test. Data are presented as mean ± SEM unless otherwise indicated (not significant, $P > 0.05$; $^*P < 0.05$; $^{**}P < 0.01$; $^{***}P < 0.001$, $^{****}P < 0.0001$). Labeled neurons and spines were reconstructed using the Neurolucida tracing program (MBF Bioscience).

1. Fernández ME, Croce S, Boutin C, Cremer H, Raineteau O (2011) Targeted electroporation of defined lateral ventricular walls: A novel and rapid method to study fate specification during postnatal forebrain neurogenesis. *Neural Dev* 6:13.

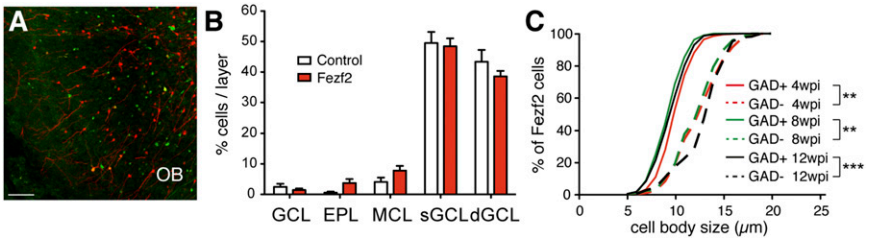

Fig. S1. Fezf2 expression did not alter the cell distribution in the olfactory bulb (OB). (*A*) Proportion and location of control (red) and Fezf2 (green) cells that reached the OB were similar. (Scale bar: 50 μm.) (*B*) Bar graph illustrates a similar distribution of control and $Fezf2^+$ neurons in different layers of the OB 4 wk postinjection (wpi) (mean ± SEM; two-way ANOVA; $P > 0.05$, Bonferroni multiple comparison post hoc test). dGCL, deep granule cell layer; EPL, external plexiform layer; GCL, glomerular cell layer; MCL, mitral cell layer; sGCL, superficial granule cell layer. (*C*) Cumulative frequency distribution of $Fezf2^+$ neurons showing that $Fezf2^+$/glutamic acid decarboxylase (GAD) 67^- neurons have a larger cell body at different time points after injection [bin width = 0.2 μm; Kolmogorov–Smirnov (K-S) test: $^{**}P = 0.0061$ for 4 wpi ($n = 10$ mice); $^{**}P = 0.0018$ for 8 wpi ($n = 5$ mice); $^{***}P < 0.001$ for 12 wpi ($n = 6$ mice)].

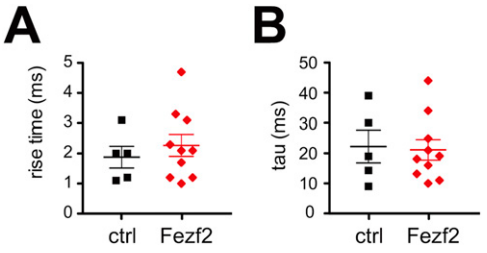

Fig. S2. Brief voltage steps elicited currents in SVZ-derived control (tdTomato) or $Fezf2^+$ neurons with a similar rise time (*A*; *t* test, $P > 0.05$) and decay time (tau, *B*; *t* test, $P > 0.05$). ctrl, control.

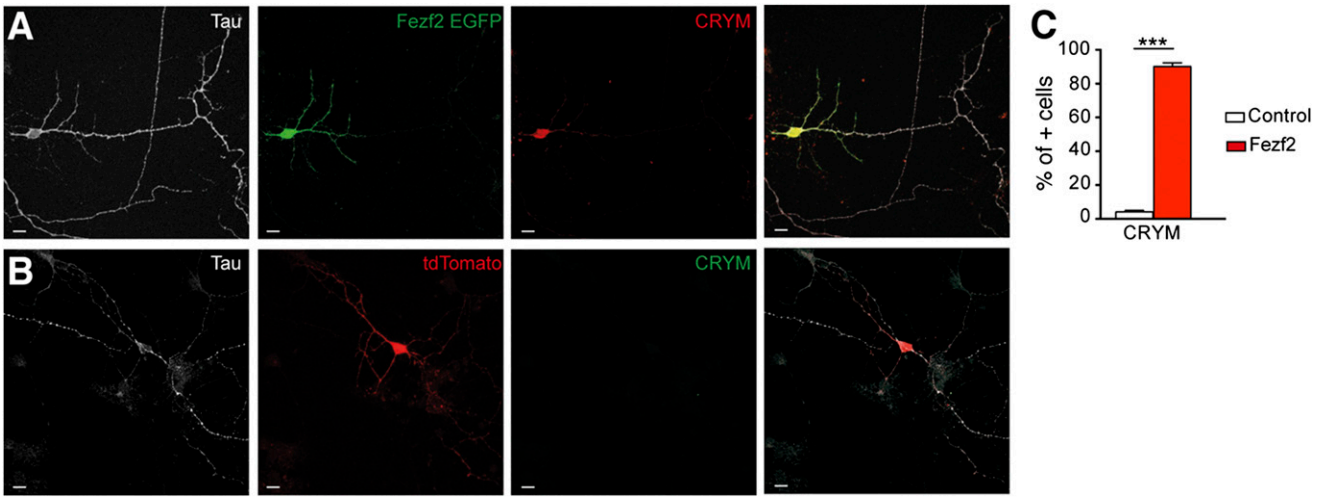

Fig. S3. (*A*) Neurosphere-derived Fezf2$^+$ neurons (green) positive for the neuronal marker tau (white) express the corticofugal pyramidal neuron marker CRYM (red) 3 d after neurosphere differentiation. (Scale bars: 10 μm.) (*B*) Control neurons (tdTomato, red) positive for the neuronal marker tau (white) do not express CRYM (green). (Scale bars: 10 μm.) (*C*) Total of 90.1 ± 2.21% of Fezf2$^+$ neurons and 4.09 ± 0.97% of control neurons are CRYM$^+$ (n = 3 neurosphere preparations; n = 264 Fezf2$^+$ cells vs. n = 356 control neurons, t test ***$P < 0.001$).

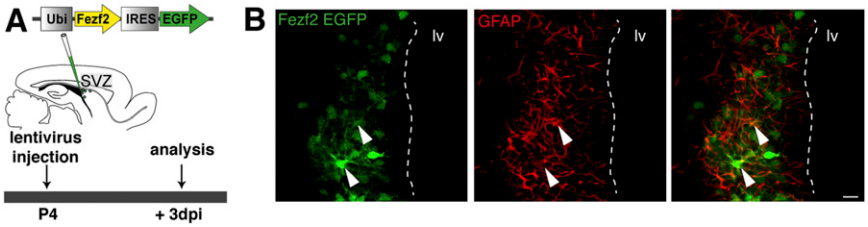

Fig. S4. Lentivirus expression in stem cells 3 d after injection. (*A*) Schematic representation of Fezf2 lentivirus injection into the SVZ of P4 mice, analyzed 3 dpi. (*B*) White arrows indicate Fezf2-GFP (green) expression in GFAP$^+$ cells (red, stem cells) in the SVZ. lv, lateral ventricle. (Scale bar: 20 μm.)

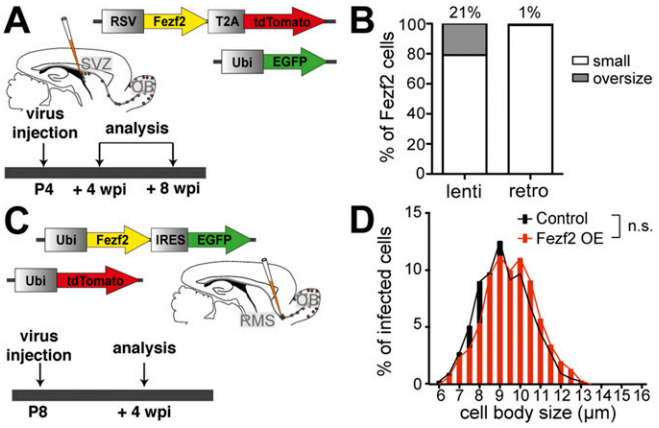

Fig. S5. Fezf2 specifically alters the differentiation of neural stem cells. (*A*) Retroviruses expressing EGFP and Fezf2-tdTomato were injected into the SVZ of P4 mice and analyzed 4 (n = 8 mice) and 8 (n = 4 mice) wpi. (*B*) Although lentiviral injections yield 21% oversized cells, retroviral injections yield only 1% (three of 289 cells; Fisher's exact test, $P < 0.001$). (*C*) Fezf2-EGFP and tdTomato expressing lentivirus were injected into the rostral migratory stream (RMS) of P8 mice to infect neuroblasts and analyzed 4 wpi (n = 8 mice). (*D*) Frequency distribution of cell body size of control and Fezf2$^+$ cells was similar (bin width = 0.5 μm; K-S test: P = 0.999). n.s., not significant.

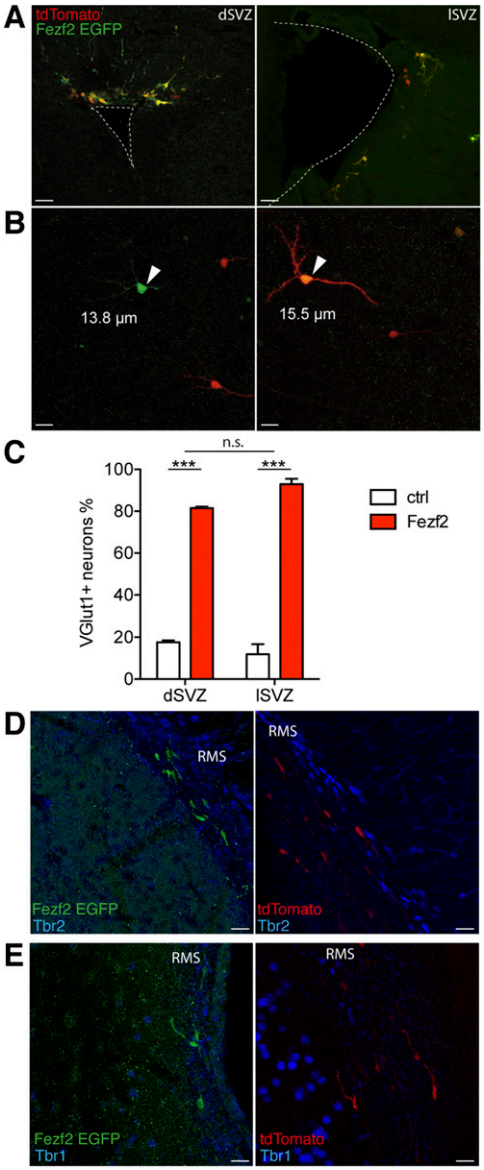

Fig. S6. Fezf2 does not specifically respecify a subpopulation of stem cells residing in the dorsal SVZ (dSVZ). Specific electroporation of Fezf2-GFP and tdTomato plasmid in the dSVZ (*A*, *Left*) or lateral SVZ (lSVZ) (*A*, *Right*) led to oversized Fezf2 cells in the OB (arrowheads in *B*) in both cases. (Scale bars: *A*, 50 μm; *B*, 20 μm.) (*C*) Total of 81.57 ± 0.65% of Fezf2$^+$ neurons and 17.60 ± 0.92% of ctrl neurons derived from the dSVZ are VGlut1$^+$ (n = 2 neurosphere preparations, n = 44 Fezf2$^+$ cells vs. n = 26 control neurons), and, similarly, 92.95 ± 2.59% of Fezf2$^+$ neurons and 11.86 ± 4.81% of ctrl neurons derived from the lSVZ are VGlut1$^+$ (n = 2 neurosphere preparations, n = 54 Fezf2$^+$ cells vs. n = 64 ctrl neurons) as measured by two-way ANOVA with a Bonferroni multiple comparison post hoc test: ctrl vs. Fezf2, ***$P < 0.0001$; dSVZ vs. lSVZ, n.s.. Fezf2 (EGFP) or control (tdTomato) migrating neuroblasts in the RMS are Tbr2$^-$ (*D*) and Tbr1$^-$ (*E*). (Scale bars: 20 μm.)

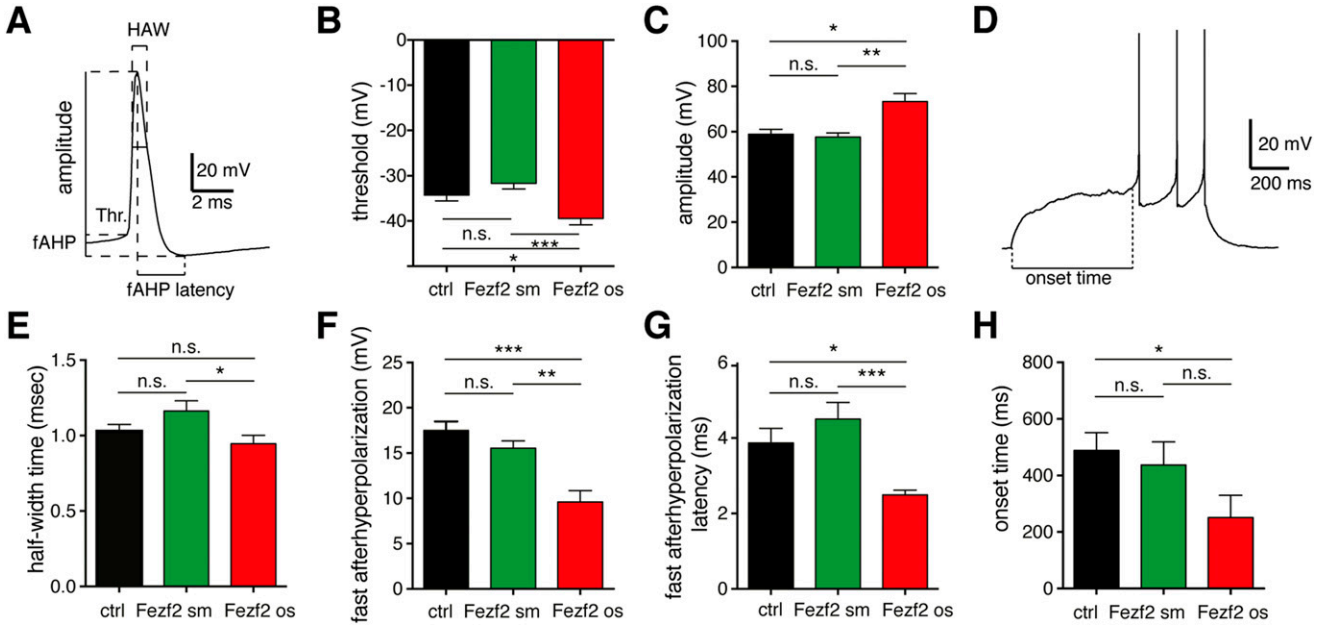

Fig. S7. (*A*) Analysis of action potential (AP) waveforms, as exemplified. (*B*) AP threshold [ctrl vs. Fezf small (sm): $P > 0.05$; ctrl vs. Fezf2 oversized (os): $^{*}P < 0.05$; Fezf2 sm vs. Fezf2 os: $^{***}P < 0.001$]. (*C*) AP amplitude (ctrl vs. Fezf sm: $P > 0.05$; ctrl vs. Fezf2 os: $^{*}P < 0.05$; Fezf2 sm vs. Fezf2 os: $^{**}P < 0.01$). (*E*) Half-width (ctrl vs. Fezf sm: $P > 0.05$; ctrl vs. Fezf2 os: $P > 0.05$; Fezf2 sm vs. Fezf2 os: $^{*}P < 0.05$). (*F*) Fast after hyperpolarization (ctrl vs. Fezf sm: $P > 0.05$; ctrl vs. Fezf2 os: $^{***}P < 0.001$; Fezf2 sm vs. Fezf2 os: $^{**}P < 0.001$). (*G*) Fast after hyperpolarization latency (ctrl vs. Fezf sm: $P > 0.05$; ctrl vs. Fezf2 os: $^{*}P < 0.05$; Fezf2 sm vs. Fezf2 os: $^{***}P < 0.001$). The time of onset (*H*) was defined as the time of the first AP in the train recorded at the lowest current pulse injection eliciting APs and measured from the start of current injection (*D*) (ctrl vs. Fezf sm: $P > 0.05$; ctrl vs. Fezf2 os: $^{*}P < 0.05$; Fezf2 sm vs. Fezf2 os: $P > 0.05$). fAHP, fast afterhyperpolarization, HAW, half-width, Thr., threshold. (Statistical analysis was performed using the Kruskal–Wallis test followed by Dunn's test, except for *E*, where one-way ANOVA followed by Tukey's test was used).

Table S1. Fezf2 modifies the synaptic input onto OB granule cells towards a pyramidal phenotype

	mIPSC decay time constant, ms	mEPSC decay time constant, ms
Control olfactory bulb granule cells, present study	14.9 ± 1.1	3.8 ± 0.7
Previously reported for olfactory bulb granule cells	16.8 ± 7.1 (1)	2.1 (fast kinetics) and 9.2 (slow kinetics) (1) 1.5 ± 0.1 (fast kinetics, 72% of mEPSCs) (3) 5.7 ± 0.3 (slow kinetics, 28% of mEPSCs) (i.e., $\tau_{weighted}$ = 2.77 ms) (3)
Fezf2^{+} respecified cells, present study	8.6 ± 1.0	6.8 ± 0.6
Previously reported for layer 5 pyramidal cells	7.5 ± 0.32 (2)	4.28 ± 0.12 (somatosensory cortex, 4- to 5-wk-old mice) (2) 4.4 ± 0.3 (visual cortex, P13–P20 mice) (4) 8.0 ± 0.6 (prefrontal cortex, adult rats) (5)

1. Carleton A, Petreanu LT, Lansford R, Alvarez-Buylla A, Lledo PM (2003) Becoming a new neuron in the adult olfactory bulb. *Nat Neurosci* 6(5):507–518.
2. Dani VS, et al. (2005) Reduced cortical activity due to a shift in the balance between excitation and inhibition in a mouse model of Rett syndrome. *Proc Natl Acad Sci USA* 102(35):12560–12565.
3. Schoppa NE (2006) AMPA/kainate receptors drive rapid output and precise synchrony in olfactory bulb granule cells. *J Neurosci* 26(50):12996–13006.
4. Madara JC, Levine ES (2008) Presynaptic and postsynaptic NMDA receptors mediate distinct effects of brain-derived neurotrophic factor on synaptic transmission. *J Neurophysiol* 100(6):3175–3184.
5. Counotte DS, et al. (2011) Lasting synaptic changes underlie attention deficits caused by nicotine exposure during adolescence. *Nat Neurosci* 14(4):417–419.